



Prognostic Stratification Based on HIF-1 Signaling for Evaluating Hypoxic Status and Immune Infiltration in Pancreatic Ductal Adenocarcinomas

OPEN ACCESS

Edited by:

Yunfei Xu,
Shandong University, China

Reviewed by:

Qianjin Liao,
Central South University, China
M. Celeste Simon,
University of Pennsylvania,
United States

*Correspondence:

Baohua Hou
15917919681@163.com
Yajin Chen
cyj0509@126.com
Chuanzhao Zhang
zhangchuanzhao@gdph.org.cn

†These authors have contributed
equally to this work

Specialty section:

This article was submitted to
Cancer Immunity
and Immunotherapy,
a section of the journal
Frontiers in Immunology

Received: 07 October 2021

Accepted: 19 November 2021

Published: 03 December 2021

Citation:

Zhuang H, Wang S, Chen B, Zhang Z,
Ma Z, Li Z, Liu C, Zhou Z, Gong Y,
Huang S, Hou B, Chen Y and Zhang C
(2021) Prognostic Stratification
Based on HIF-1 Signaling for
Evaluating Hypoxic Status and
Immune Infiltration in Pancreatic
Ductal Adenocarcinomas.
Front. Immunol. 12:790661.
doi: 10.3389/fimmu.2021.790661

Hongkai Zhuang^{1,2†}, Shujie Wang^{1†}, Bo Chen^{3†}, Zedan Zhang^{4†}, Zuyi Ma¹,
Zhenchong Li¹, Chunsheng Liu¹, Zixuan Zhou¹, Yuanfeng Gong¹, Shanzhou Huang¹,
Baohua Hou^{1*}, Yajin Chen^{2*} and Chuanzhao Zhang^{1*}

¹ Department of General Surgery, Guangdong Provincial People's Hospital, Guangdong Academy of Medical Sciences, Guangzhou, China, ² Department of Hepatobiliary Surgery, Sun Yat-Sen Memorial Hospital, Sun Yat-Sen University, Guangzhou, China, ³ Department of Breast Cancer, Cancer Center, Guangdong Provincial People's Hospital, Guangdong Academy of Medical Sciences, Guangzhou, China, ⁴ Department of Urology, Peking University First Hospital, Beijing, China

Pancreatic ductal adenocarcinoma (PDAC) has a hypoxic and desmoplastic tumor microenvironment (TME), leading to treatment failure. We aimed to develop a prognostic classifier to evaluate hypoxia status and hypoxia-related molecular characteristics of PDAC. In this study, we classified PDAC into three clusters based on 16 known hypoxia-inducible factor 1 (HIF-1)-related genes. Nine differentially expressed genes were identified to construct an HIF-1 score system, whose predictive efficacy was evaluated. Furthermore, we investigated oncogenic pathways and immune-cell infiltration status of PDAC with different scores. The C-index of the HIF-1 score system for OS prediction in the meta-PDAC cohort and the other two validation cohorts were 0.67, 0.63, and 0.65, respectively, indicating that it had a good predictive value for patient survival. Furthermore, the area under the curve (AUC) of the receiver operating characteristic (ROC) curve of the HIF-1 score system for predicting 1-, 3-, and 4-year OS indicated the HIF-1 score system had an optimal discrimination of prognostic prediction for PDAC. Importantly, our model showed superior predictive ability compared to previous hypoxia signatures. We also classified PDAC into HIF-1 scores of low, medium, and high groups. Then, we found high enrichment of glycolysis, mTORC1 signaling, and MYC signaling in the HIF-1 score high group, whereas the cGMP metabolic process was activated in the low score group. Of note, analysis of public datasets and our own dataset showed a high HIF-1 score was associated with high immunosuppressive TME, evidenced by fewer infiltrated CD8⁺ T cells, B cells, and type 1 T-helper cells and reduced cytolytic activity of CD8⁺ T cells. In summary, we established a specific HIF-1 score system to discriminate

PDAC with various hypoxia statuses and immune microenvironments. For highly hypoxic and immunosuppressive tumors, a combination treatment strategy should be considered in the future.

Keywords: PDAC, HIF-1, hypoxia, ICB, immunosuppression, immune infiltration

INTRODUCTION

Pancreatic ductal adenocarcinoma (PDAC) is one of the deadliest malignancies and accounts for nearly 4.5% of all cancer-related deaths worldwide, with a 5-year survival rate of less than 10% (1, 2). Despite major efforts to improve the diagnosis and treatment of PDAC, the survival rate of patients with PDAC has not significantly improved (3). In particular, novel treatments were found to have limited indications or low response rates (2–5). For example, olaparib, is only effective in patients with germline BRCA mutations (6–8). PD-1/PD-L1 inhibition-based immunotherapy is under investigation, and preliminary data showed limited efficacy for single drug treatment (9, 10). These are due to tumor heterogeneity and the specific tumor microenvironment (TME) in PDAC (11–13). In addition, the traditional prognostic clinicopathological characteristics, such as American Joint Committee on Cancer (AJCC) stage and histologic grade, have less accurate predictive value for the clinical outcome of patients with PDAC (14–16). Therefore, exploring the molecular classification and mechanisms leading to TME development and tumor progression will help in designing more effective precision treatments for PDAC.

Desmoplasia and hypoxia are the major characteristics of TME in PDAC, in which desmoplasia worsens tumor hypoxia, and hypoxic conditions promote the proliferation of stromal cells such as CAFs, leading to severe desmoplasia (17–19). Hypoxia-inducible factor-1 (HIF-1) is a master regulator of tumor hypoxia and plays a critical role in promoting the malignant phenotypes of PDAC (20, 21). For example, HIF-1 was reported to enhance the transcription of Snail by binding to its hypoxia response elements, inducing epithelial-mesenchymal transition and cancer metastasis in PDAC (22). In addition, the hypoxic TME of PDAC could upregulate the expression of multidrug resistance 1 (MDR1) through the HIF-1 signaling pathway, thereby mediating chemotherapy resistance (23). Importantly, HIF-1 regulates anti-tumor immunity by regulating the expression of PD-L1 or CD47, resulting in an immunosuppressive TME (24–27). Thus, hypoxia and HIF-1 may affect the expression of different genes and lead to corresponding cancer cell behaviors. Therefore, it is of great interest to establish a prognostic classifier to evaluate the different hypoxia status and characteristics of hypoxia-related subtypes of PDAC.

In the current study, using multiple bioinformatics analysis, we classified patients with PDAC into three clusters based on HIF-1 related genes. Nine differentially expressed genes among the three HIF-1 clusters were identified from the meta-PDAC cohort to construct an HIF-1 score system for prognostic

stratification of patients with PDAC. The predictive efficacy of the HIF-1 score system was evaluated in meta-PDAC cohort and validation cohort. Of note, we also comprehensively assessed the oncologic biological pathways and immune-cell infiltration status for pancreatic cancers with different HIF-1 scores.

MATERIALS AND METHODS

PDAC Datasets and Preprocessing

Publicly available PDAC mRNA-sequencing data and corresponding clinical information of patients were obtained from the Gene Expression Omnibus (GEO, <https://www.ncbi.nlm.nih.gov/geo/>), the Cancer Genome Atlas (TCGA, <https://cancergenome.nih.gov/>), and the International Cancer Genome Consortium (ICGC, <https://icgc.org/>) databases. The PDAC dataset GSE62452 (Platform: GPL6244; 61 non-tumor samples and 69 tumor samples) from the GEO database and TCGA PDAC dataset (4 non-tumor samples and 146 tumor samples) were integrated into a meta-PDAC cohort (65 non-tumor samples and 215 tumor samples). The R package ‘sva’ was used to eliminate batch effects. Of the 215 PDAC cases in the meta-PDAC cohort, 205 were cases with OS > 1 month and were used as the training cohort for prognostic stratification based on HIF-1 signaling. Transcriptomic data from the ICGC PDAC cohort (N = 96; validation cohort 1) and GSE79668 cohorts (Platform: GPL11154; N = 51; validation cohort 2) were used for validation.

Identification of HIF-1 Related Genes in PDAC

A total of 16 HIF-1 related genes were identified, corroborating previous studies (28, 29). The differential expression of these genes between non-tumor and tumor samples was evaluated in the meta-PDAC cohort. The prognostic value of HIF-1-related genes in PDAC was evaluated in a meta-PDAC cohort using Kaplan–Meier (KM) survival analysis.

Consensus Clustering Analysis

Using the R package ‘ConsensusClusterPlus’, consensus clustering was conducted to categorize PDAC patients into subgroups based on the expression of HIF-1 related genes. Principal component analysis (PCA) was performed to evaluate the clustering efficacy. KM survival analysis was then performed to assess the OS difference between different subgroups. The differential expression of HIF-1 related genes between different subgroups was visualized using the R package ‘pheatmap’. Then, the association between subgroups and clinicopathological characteristics, including AJCC stage and

histologic grade, was evaluated using the chi-square test or Fisher's exact test. Differentially expressed genes between different subgroups were identified using the R package 'limma' under the threshold of $|\log_2 \text{fold change (FC)}| > 0.5$. The overlapping differentially expressed genes (ODEGs) were selected for subsequent analysis.

Development and Validation of the HIF-1 Score System

Using the R package 'survival', we performed univariate Cox regression analysis to assess the association between the ODEGs and OS in batches in the meta-PDAC cohort. Then, using the R package 'glmnet', the critical prognosis-associated ODEGs were further determined through least absolute shrinkage and selection operator (LASSO) regression analysis. KM survival analysis was also conducted to evaluate the prognostic association of the critical prognosis-associated ODEGs according to the optimal cutoff point using the R package 'survminer'. Using the R package 'survival', an HIF-1 score system was developed based on a linear combination of the expression of the critical prognosis-associated ODEGs and the multivariable Cox regression coefficients as the weight. For external validation of the HIF-1 score system, the HIF-1 score was also calculated for patients with PDAC in the ICGC PDAC cohort and GSE79668 cohort with the same multivariable Cox regression coefficients in the meta-PDAC cohort.

Using the R package 'survminer', KM survival curves for OS were constructed according to the optimal cutoff points obtained from X-tile software version 3.6.1 (low HIF-1 score, medium HIF-1 score, and high HIF-1 score) (30). The predictive performance of the HIF-1 score system was evaluated using the C-index and AUC of the ROC curves. PCA was performed to evaluate prognostic stratification efficacy. In addition, the association between HIF-1 score and clinicopathological characteristics, including AJCC stage and histologic grade, was evaluated using the chi-square test.

Association Between HIF-1 Score and Somatic Mutation in PDAC

Using the R package 'maftools', we visualized the somatic mutation profile of PDAC in the TCGA PDAC cohort. We further investigated the association between HIF-1 score and somatic mutation using the chi-square test. We also assessed the association between tumor mutation burden (TMB) and HIF-1 score. In summary, we aimed at preliminarily determining whether somatic mutation status affected hypoxia status in PDAC.

Gene Set Variation Analysis (GSVA)

GSVA is an analytical method used to calculate the enrichment scores of specific gene sets for each sample based on RNA-seq (31). Using the R package 'gsva', we conducted GSVA to estimate the enrichment scores of 50 gene ontology gene sets (h.all.v7.0.symbols.gmt), and 231 metabolic process gene sets (c5.go.bp.v7.4.symbols.gmt) obtained from the Molecular Signature Database (MSigDB, <http://software.broadinstitute.org/gsea/msigdb>) in the meta-PDAC cohort. Furthermore, GSVA was also implanted to calculate the enrichment scores of 25 immune-related terms extracted from previous studies (32).

org/gsea/msigdb) in the meta-PDAC cohort. Furthermore, GSVA was also implanted to calculate the enrichment scores of 25 immune-related terms extracted from previous studies (32).

Association Between HIF-1 Score and Hypoxia Scores

A total of three hypoxia scores based on the TCGA PDAC dataset were obtained from the cBioportal database (<http://www.cbioportal.org/>), including Buffa hypoxia, Ragnum hypoxia score, and Winter hypoxia score (33–35). We then evaluated the differences in these three hypoxia scores between different HIF-1 score subgroups. Correlation analysis between the HIF-1 score and these three hypoxia scores was conducted using Pearson correlation coefficients. KM survival curves were obtained for HIF-1 and the three hypoxia scores in the sample TCGA PDAC cohort. Then, ROC curves for 1-, 2-, and 3-year OS were performed for HIF-1 score and these three hypoxia scores to compare their predictive reliability for OS.

Real-Time Polymerase Chain Reaction (RT-qPCR)

A total of 28 samples of PDAC patients were collected after surgical resection in Guangdong Provincial People's Hospital during 2015–2021. The total mRNA of PDAC tissues were isolated using TRIzol (Invitrogen, USA) following the manufacturer's instruction. The RT-qPCR was conducted in triplicate using Taqman™ Assay kit (Applied Biosystems, USA). The expressions were estimated by $2^{-\Delta\Delta C_t}$ method and β -actin was used as an internal control. The sequences of primers for the nine genes of our model were shown in **Table S1**. Informed consent was obtained from all patients, and the study was approved by the Ethics Committee of Guangdong Provincial People's Hospital.

Immunohistochemistry

The formalin-fixed paraffin-embedded sections (4- μ m thick) from the corresponding PDAC samples were deparaffinized and rehydrated, followed by antigen retrieval using citrate buffer (pH 8.0). Staining for CD8+ T cells were performed using a rabbit anti-CD8A monoclonal antibody (GB13429, Servicebio, China) and the LSAB+ System HRP kit (DAKO, Carpinteria, CA) according to the manufacturer's instructions. The levels of CD8A-positive cells was quantified by whole slide digital scanning using Aperio VERSA scanner (Leica Biosystems, USA), and converted to number/mm².

Statistical Analysis

GraphPad Prism 8.0 software (GraphPad Software, Inc.) and the R software version 3.5.2 (<http://r-project.org/>) were used to conduct all statistical analyses. Group differences analysis were performed using Wilcoxon test or Kruskal–Wallis test, and expressed as means \pm standard deviation (SD). Pearson correlation coefficient was used for correlation analysis. A two-sided P value < 0.05 was considered as statistically significant.

RESULTS

The mRNA Expression of HIF-1 Related Genes in PDAC

We analyzed 16 known HIF-1 related genes and found that 15 were significantly overexpressed in tumor samples in the meta-PDAC cohort, including *ALDOA*, *ALDOC*, *ENO1*, *GAPDH*, *HIF1A*, *HK1*, *HK2*, *LDHA*, *PDK1*, *PFKFB3*, *PFKL*, *PGK1*, *PKM*, *SLC2A1*, and *SLCS2A3*, whereas only one (*BNIP3*) was significantly downregulated (**Figure S1A**). KM survival analysis demonstrated that 13 HIF-1 related genes were significantly associated with shorter OS of PDAC patients, namely *ALDOA*, *ALDOC*, *ENO1*, *GAPDH*, *HIF1A*, *HK1*, *HK2*, *LDHA*, *PDK1*, *PGK1*, *PKM*, *SLC2A1*, and *SLCS2A3*. (**Figure S1B**).

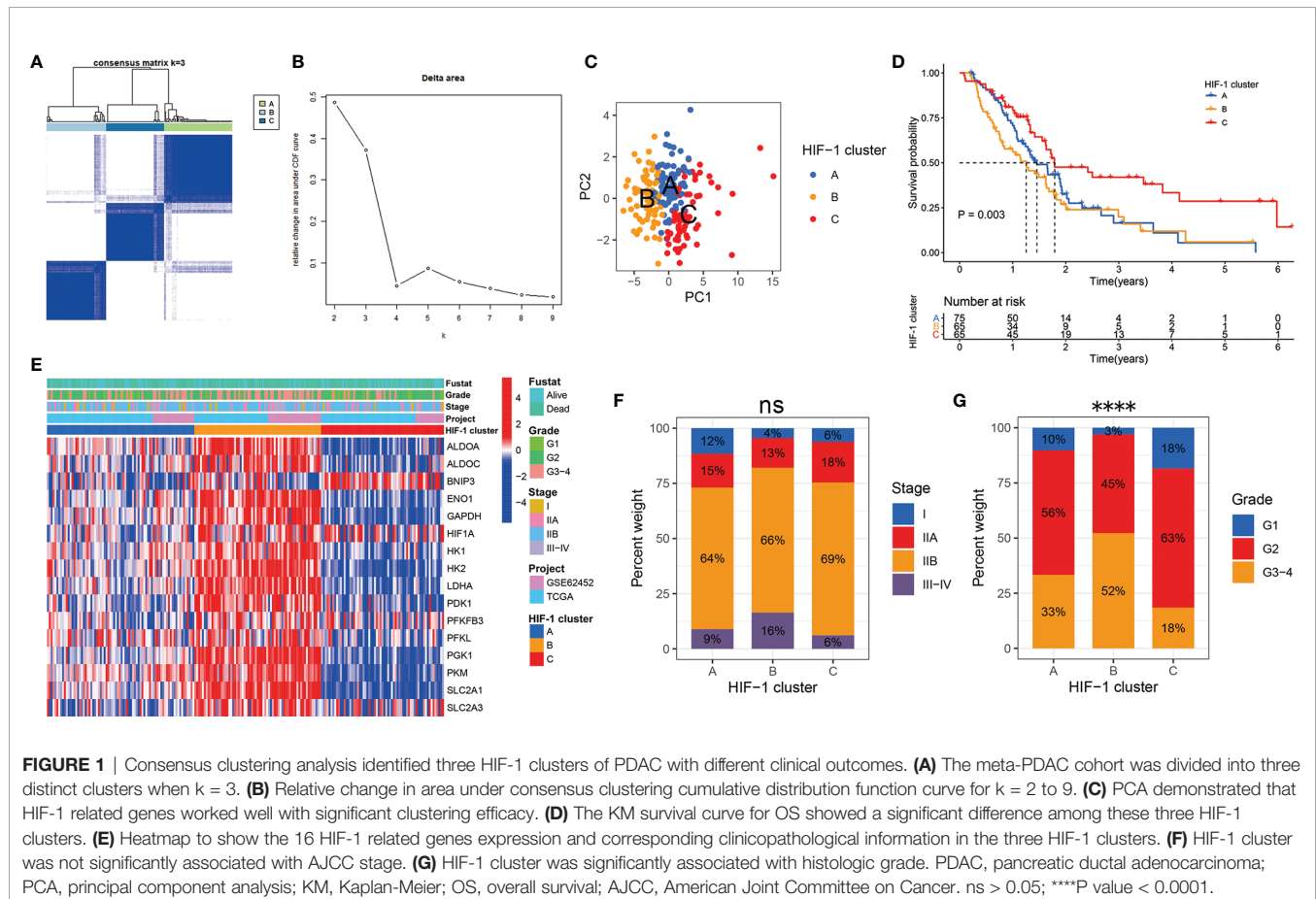
Consensus Clustering Analysis Identified Three HIF-1 Clusters of PDAC With Different Clinical Outcomes

According to the mRNA expression similarity of HIF-1 related genes, $k = 3$ was the most appropriate choice for classifying patients with PDAC into three clusters, namely HIF-1 clusters A, B, and C (**Figures 1A, B**). PCA demonstrated that HIF-1 related genes worked well with significant clustering efficacy (**Figure 1C**). The KM survival curve for OS showed that HIF-1 cluster C had the best survival, and HIF-1 cluster B had shorter

medium OS than HIF-1 cluster A, though survival differences between cluster A and cluster B was not statistically significant (**Figure 1D**). A heatmap was constructed to visualize the distribution of these 16 HIF-1 related genes, AJCC stage, and the histologic grade among the three HIF-1 clusters (**Figure 1E**). Furthermore, we found that the HIF-1 cluster was not significantly associated with AJCC stage but significantly associated with histologic grade (**Figures 1F, G**), in which HIF-1 cluster B was significantly correlated with advanced histologic grade and HIF-1 cluster C was correlated with low histologic grade. These results indicate that different HIF-1 clusters are associated with different clinical outcomes.

Development and Validation of the HIF-1 Score System

The DEGs between different HIF-1 clusters were visualized using volcano plots (**Figures S2A–C**). There were 249 ODEGs among the three HIF-1 clusters (**Figure S2D**). Univariable Cox regression analysis demonstrated that 130 ODEGs were significantly associated with OS of patients with PDAC ($P < 0.05$) (**Table S2**). Moreover, LASSO regression analysis identified nine critical prognosis-associated ODEGs, and the KM survival analysis is shown in the forest plots (**Figure 2**). Subsequently, based on these nine critical prognosis-associated ODEGs, we constructed an HIF-1 score system using multivariable Cox



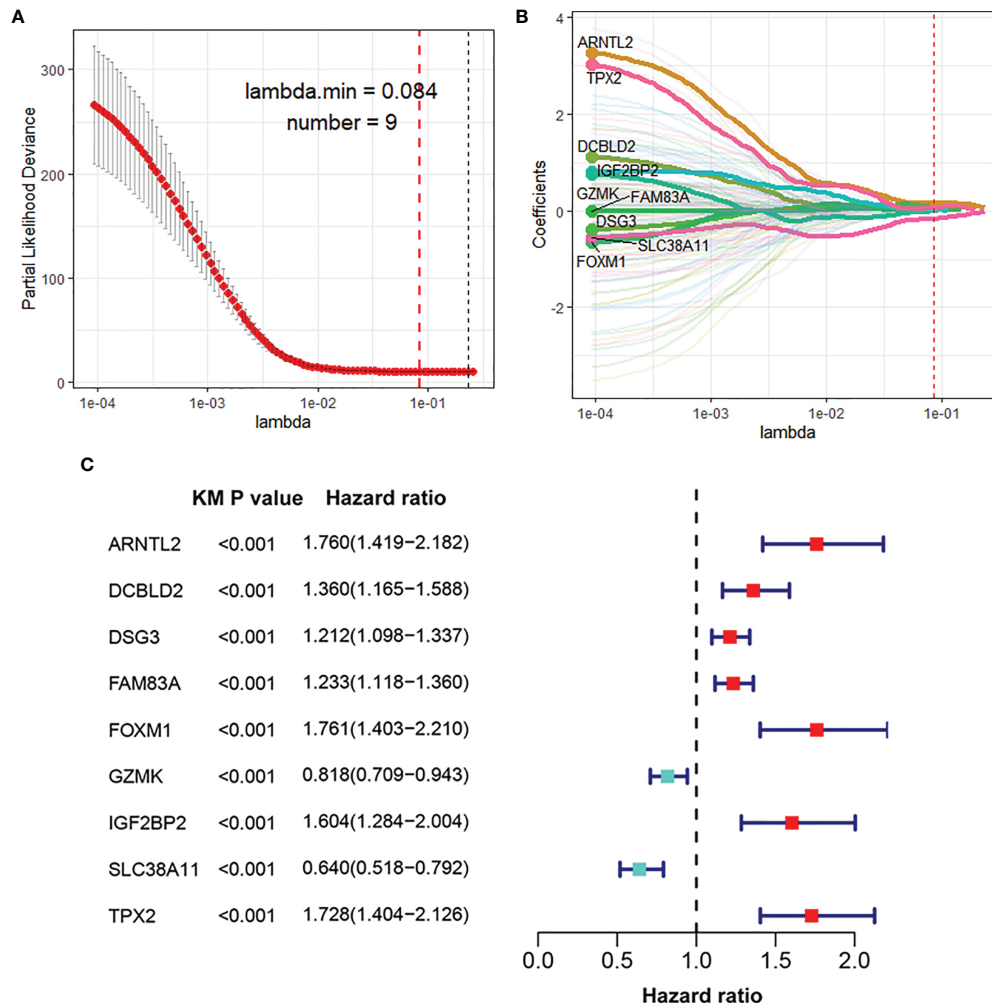


FIGURE 2 | Identification of nine critical prognosis-associated ODEGs for PDAC. **(A, B)** LASSO regression analysis identified nine critical prognosis-associated ODEGs for PDAC. **(C)** Forest plots to show the results of KM survival analysis of the nine critical prognosis ODEGs. ODEGs, overlapping differentially expressed genes; PDAC, pancreatic ductal adenocarcinoma; KM, Kaplan-Meier.

regression analysis in the meta-PDAC cohort (training cohort). The HIF-1 score was calculated by multiplying the expression of these nine critical prognosis-associated ODEGs by the corresponding multivariable Cox regression coefficients: HIF-1 score = $(0.159789 \times \text{the expression value of ARNTL2}) + (-0.005245 \times \text{the expression value of TPX2}) + (0.105759 \times \text{the expression value of DCBLD2}) + (0.045574 \times \text{the expression value of IGF2BP2}) + (-0.088258 \times \text{the expression value of GZMK}) + (-0.001925 \times \text{the expression value of FAM83A}) + (-0.245471 \times \text{the expression value of SLC38A11}) + (0.214995 \times \text{the expression value of FOXM1}) + (0.103582 \times \text{the expression value of DSG3})$. Then, we classified patients in the meta-PDAC cohort into high-, medium-, and low-HIF-1 score groups according to the optimal cutoff point obtained from X-tile 3.6.1 software (low HIF-1 score, < 1.006 ; medium HIF-1 score, $1.006 \leq & < 2.349$; high HIF-1 score, ≥ 2.349). The KM survival curves for OS showed significant differences among these three HIF-1 score subgroups,

in which the low-HIF-1 score group had the best survival and the high-HIF-1 score group had the worst survival (**Figure 3A**). For validation, HIF-1 scores were also calculated for 96 patients with PDAC in the ICGC PDAC cohort (validation cohort 1) and 51 patients with PDAC in the GSE79668 cohort (validation cohort 2). Similar results of KM survival analysis were also observed in the validation cohorts (**Figures 3B, C**).

The C-index of the HIF-1 score system for OS prediction in the meta-PDAC cohort were 0.67 (95%CI, 0.62–0.72). For validation cohorts, the HIF-1 score system also exhibited a high accuracy of OS prediction, with a C-index of 0.63 (95% CI, 0.56–0.70) in the ICGC PDAC cohort and a C-index of 0.65 (95%CI, 0.57–0.73) in the GSE79668 cohort. In addition, for the meta-PDAC cohort, the AUC values of the HIF-1 score system for predicting 1-, 2-, and 3-year OS were 0.716, 0.729, and 0.751, respectively (**Figure 3D**). Consistently, the AUC of the HIF-1 score for 1-, 2-, and 3-year OS were 0.720, 0.623, and 0.604 in the

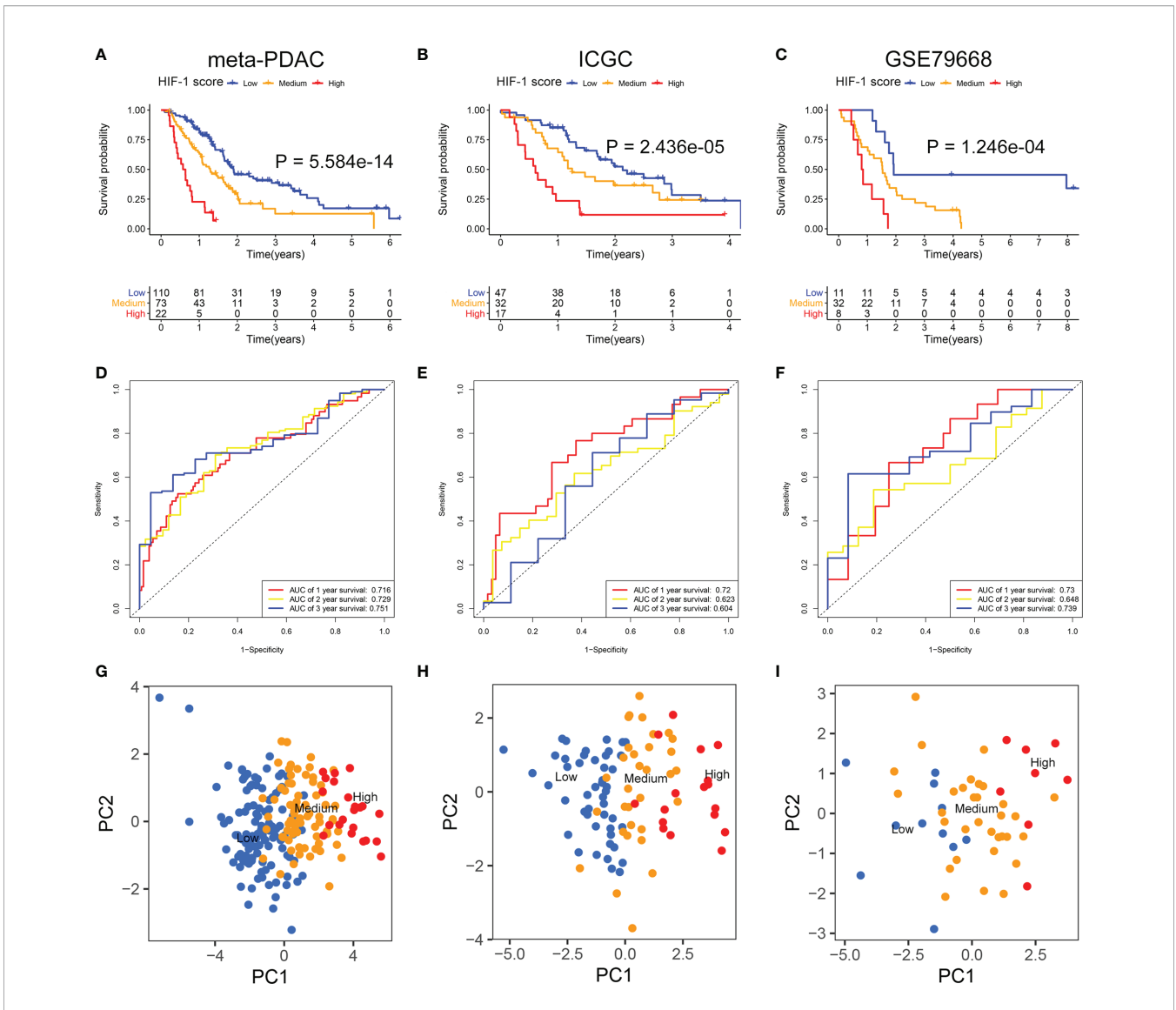


FIGURE 3 | Development and validation of the HIF-1 score system. (A–C) KM survival curves for OS of patients with PDAC according to the HIF-1 score groups in the meta-PDAC cohort, ICGC PDAC cohort, and GSE79668 cohort. (D–F) ROC curve analysis of the HIF-1 score system for 1-, 2-, and 3-year OS prediction in the meta-PDAC cohort, ICGC PDAC cohort, and GSE79668 cohort. (G–I) PCA to confirm the cluster efficacy of the HIF-1 score system in the meta-PDAC cohort, ICGC PDAC cohort, and GSE79668 cohort. KM, Kaplan-Meier; OS, overall survival; PDAC, pancreatic ductal adenocarcinoma; PCA, principal component analysis; ROC, the receiver operating characteristic curve.

ICGC PDAC cohort, and 0.730, 0.648, and 0.739 in the GSE79668 cohort, respectively (Figures 3E, F). PCA confirmed the cluster efficacy of the HIF-1 score system (Figures 3G–I). These results suggest an optimal discrimination of prognostic prediction using the HIF-1 score system for PDAC.

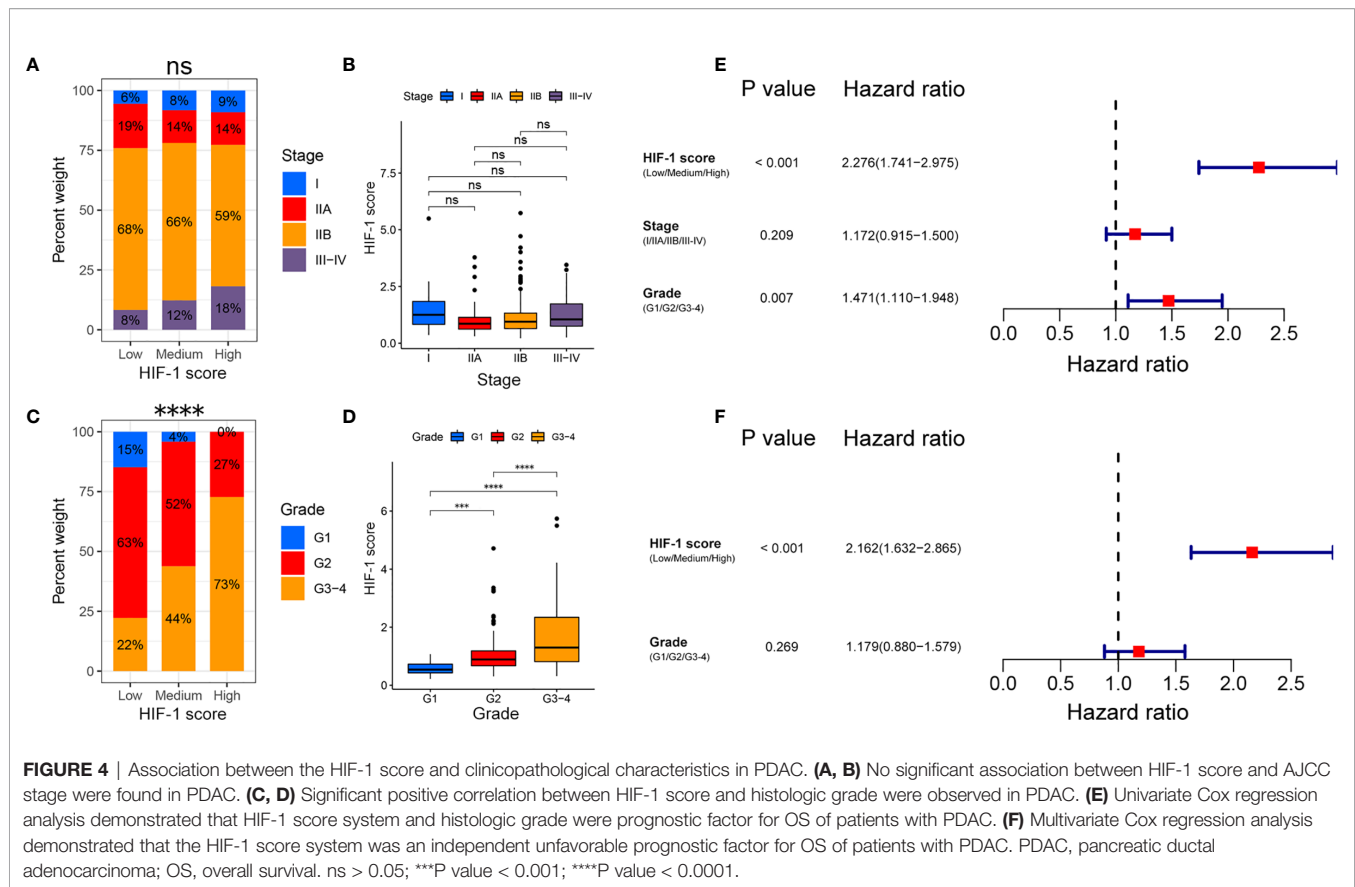
Association Between HIF-1 Score and Clinicopathological Characteristics in PDAC

Chi-square analysis indicated that the HIF-1 score system was not significantly correlated with AJCC stage in patients with PDAC, and no significant difference in HIF-1 score was found among different

AJCC stages (Figures 4A, B). However, the HIF-1 score system was significantly associated with advanced histologic grade, and PDAC patients with higher histologic grade had higher HIF-1 scores than those with lower histologic grades (Figures 4C, D). In addition, univariate and multivariate Cox regression analyses demonstrated that the HIF-1 score system was an independent prognostic factor for OS in patients with PDAC (Figures 4E, F).

Association Between HIF-1 Score and Genomic Alteration

In line with published studies, we verified that mutations in *KRAS*, *TP53*, *CDKN2A*, and *SMAD4* are four of the most



frequent genetic alterations in PDAC (Figure 5A). The most common nucleotide change was the C > T transversion (Figure 5A). Furthermore, our study revealed that *KRAS* and *TP53* mutation status were significantly correlated with the HIF-1 score (Figure 5A). Patients with *KRAS* and *TP53* alterations had significantly higher HIF-1 scores than those with wild type *KRAS* and *TP53* (Figures 5B, C). In addition, patients with higher HIF-1 scores had a much higher TMB than those with lower HIF-1 scores (Figures 5D, E).

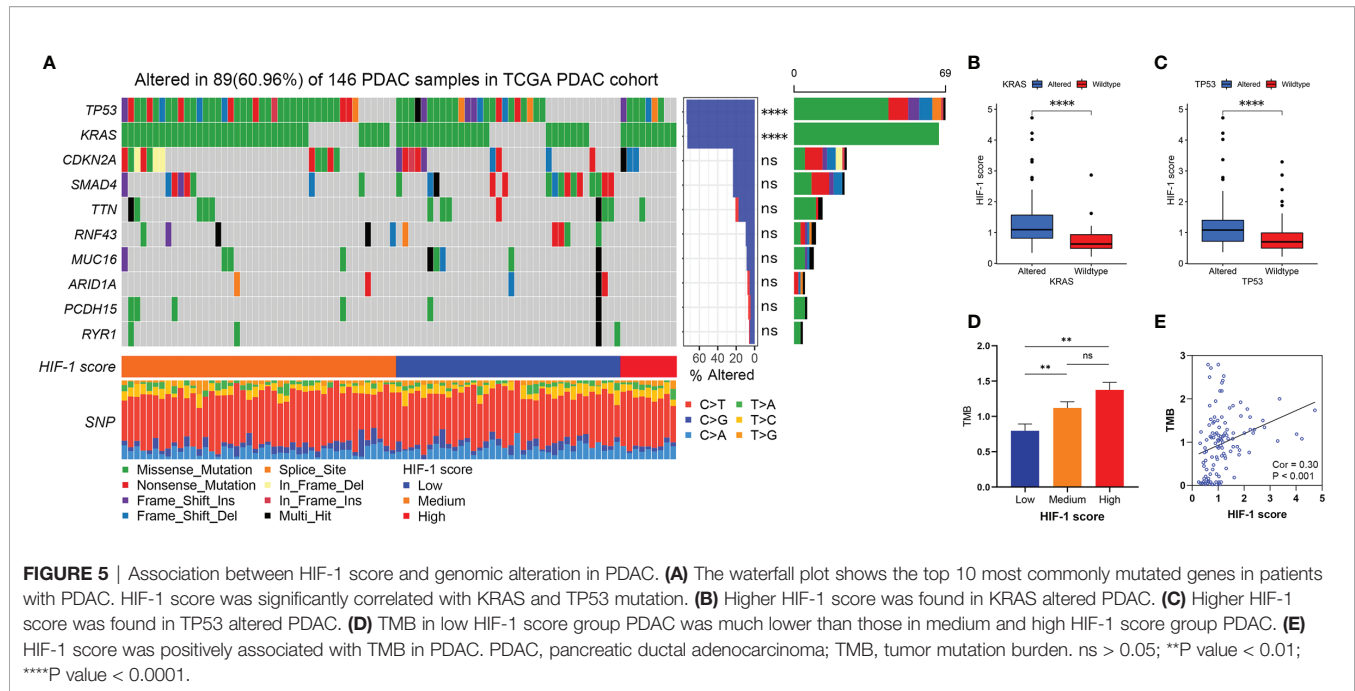
Analysis of Biological Pathways Among Different HIF-1 Score Groups

The top 20 differential oncologic biological pathways and metabolic processes between different HIF-1 score groups were presented using heatmaps (Figure S3). Ten critical oncologic biological pathways were found intersected among these three HIF-1 clusters (Figure 6A). The high HIF-1 score group had the highest enrichment scores for hypoxia, glycolysis, mTORC1 signaling, MYC signaling (MYC target V1 and MYC target V2), mitotic spindle, DNA repair, G2M targets, and E2F targets, while the low-HIF-1 score group showed the lowest enrichment. By analyzing the metabolic process, we found that the high HIF-1 score group had significant enrichment of nucleobase metabolic processes (Figure S3E, F). However, cGMP metabolic process, on the contrary, was significantly downregulated in the high HIF-1

score group but upregulated in the low-HIF-1 score group (Figure S3E).

Comparison With Our HIF-1 Score System With Other Hypoxia Score Systems

Previous studies have reported the hypoxia score system in other cancer types based on transcriptional data. In this study, we compared the predictive ability of our HIF-1 score system with these published hypoxia score systems in pancreatic cancer. First, we observed stepwise scores from HIF-1 low to high score groups calculated by the Buffa hypoxia, Ragnum hypoxia, and Winter hypoxia score systems (Figures 6B–D). These results validated our HIF-1 score system reflecting hypoxia status in pancreatic cancer. Furthermore, we found that HIF-1 score was significantly correlated with these three hypoxia score systems (Cor = 0.70, $P < 0.0001$ for Buffa hypoxia score; Cor = 0.76, $P < 0.0001$ for Ragnum hypoxia score; Cor = 0.67, $P < 0.0001$ for Winter hypoxia score) (Figures 6E–G). We then compared the prognostic stratification ability of the HIF-1 score system and these three hypoxia scores through KM survival analysis in TCGA PDAC cohort, which showed that the HIF-1 score system had the best performance in prognostic stratification (Figures 6H–K). We also compared the discriminatory ability of the HIF-1 score system and these three hypoxia scores in prognostic prediction through AUC of the ROC curves, which demonstrated that the HIF-1 score system had the best predictive efficacy for 1-, 2-, and 3-year OS of



PDAC patients (**Figures 6L–N**). These results suggest that our score system had superior predictive ability for patient prognoses.

Tumors With High HIF-1 Score Were Associated With Immunosuppressive Phenotype

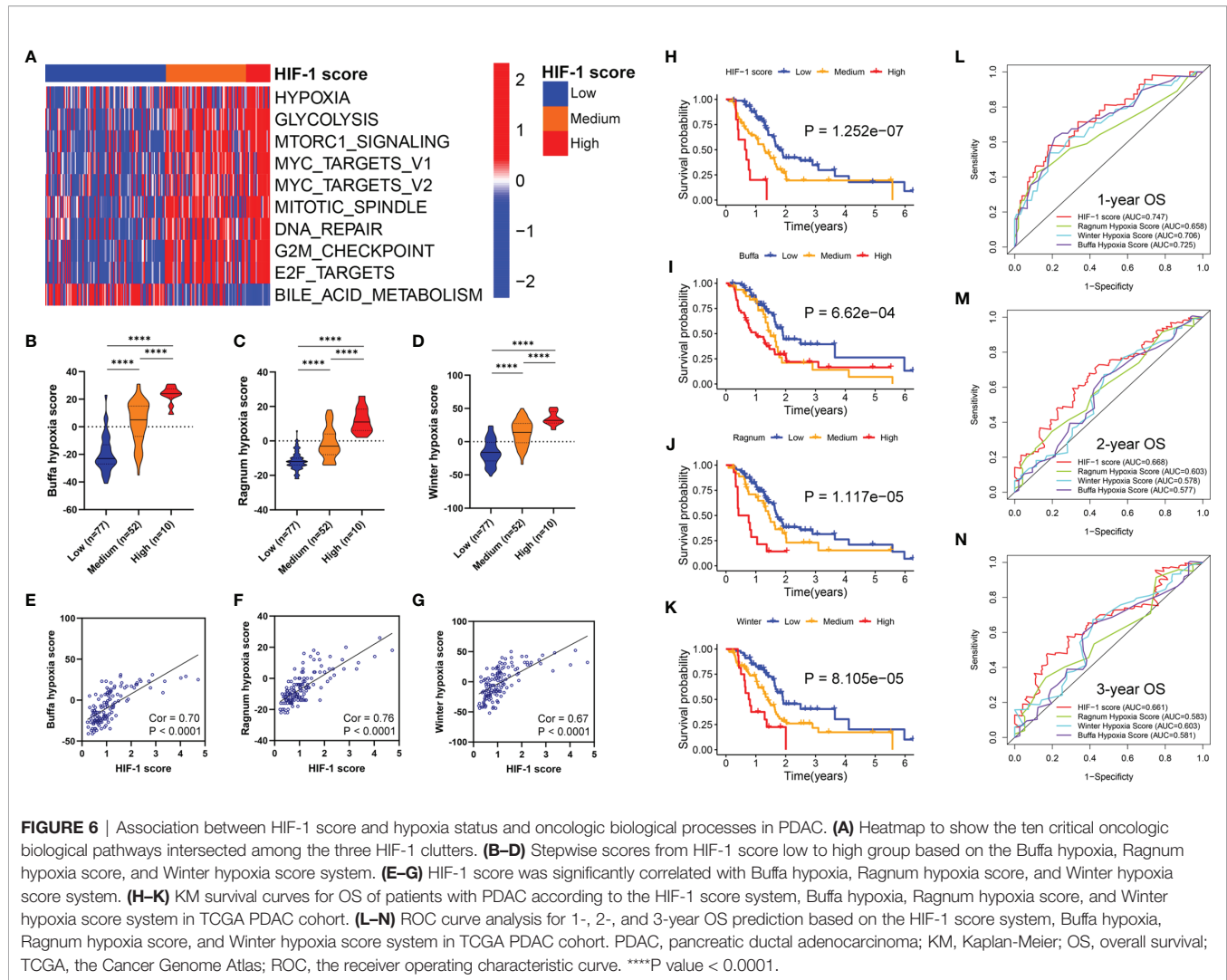
The 25 immune-related terms were visualized using a heatmap, including CD56dim natural killer cells, type-17 T-helper cells, plasmacytoid dendritic cells, gamma delta T cells, macrophages, T follicular helper cells, myeloid-derived suppressor cells, regulatory T cells, natural killer T cells, natural killer cells, activated dendritic cells, immature dendritic cells, monocytes, eosinophils, mast cells, activated CD4⁺ T cells, cytolytic activity, activated CD8⁺ T cells, tumor-infiltrating lymphocytes (TILs), type 1 T-helper cells, neutrophils, CD56bright natural killer cells, and type 2 T-helper cells (**Figure 7A**). Furthermore, significant differences in the infiltration and cytolytic activity of TILs were observed among different HIF-1 score groups, especially for activated CD8⁺ T cells, B cells (activated and immature), and type 1 T-helper cells (**Figures 7B–G**). Of note, patients in the high HIF-1 score group exhibited the lowest infiltration and cytolytic activity of CD8⁺ T cells, while those in the low-HIF-1 score group exhibited the highest (**Figures 7C, D**). To further confirm these findings, we investigated the correlation between the HIF-1 score and the infiltration of CD8⁺ T cell using our own dataset. Based on the results of RT-qPCR, we calculated the HIF-1 score for the 28 PDAC tissues, and divided them into low- and high-HIF-1 score according to the medium cutoff of HIF-1 scores. Representative image of CD8A immunostaining of low- and high-HIF-1 score PDAC samples were shown in **Figures 7H, I**. Negative association between the HIF-1 score and CD8⁺ T cell infiltration was observed (**Figure 7J**). And tumors with high HIF-1 scores exhibited

decreased infiltration of CD8⁺ T cells compared with those with low HIF-1 score (**Figure 7K**).

We also found that higher HIF-1 scores were significantly correlated with higher PD-L1 and B7-H3 expression in PDAC, which are important molecules regulating the immunosuppressive phenotype (**Figures S4A, B**). In addition, we assessed the differences in HIF-1 scores between various subtypes defined by Bailey et al., which were squamous, immunogenic, pancreatic progenitor, and aberrantly differentiated endocrine exocrine (ADEX) (36). In their study, the squamous subtype showed significantly increased hypoxia response and limited immune infiltration and the worst survival. Consistently, we found that tumors of the squamous subtype had significantly higher HIF-1 scores than those in the immunogenic subtype (“hot tumor”) (**Figure S4C**), suggesting that the squamous subtype had a highly hypoxic status. These results indicate that the HIF-1 score system might be an indicator of the immune-cell infiltration profile in PDAC. In particular, our results suggest an immunosuppressive status of tumors with high HIF-1 score (“cold tumor”).

DISCUSSION

PDAC is one of the most lethal malignancies with a heterogeneous molecular profile and various hypoxic TMEs (13, 37–39). Over the past decade, molecular target therapy and immune checkpoint inhibitors have been breakthrough advancements in the treatment of various malignancies, such as non-small cell lung cancer, hepatocellular carcinoma, and melanoma (40–42). However, limited therapeutic efficacy has been observed in PDAC due to the limited infiltration of anti-tumor immune cells in the hypoxic TME (43–45). Indeed, the hypoxic TME of PDAC contributes

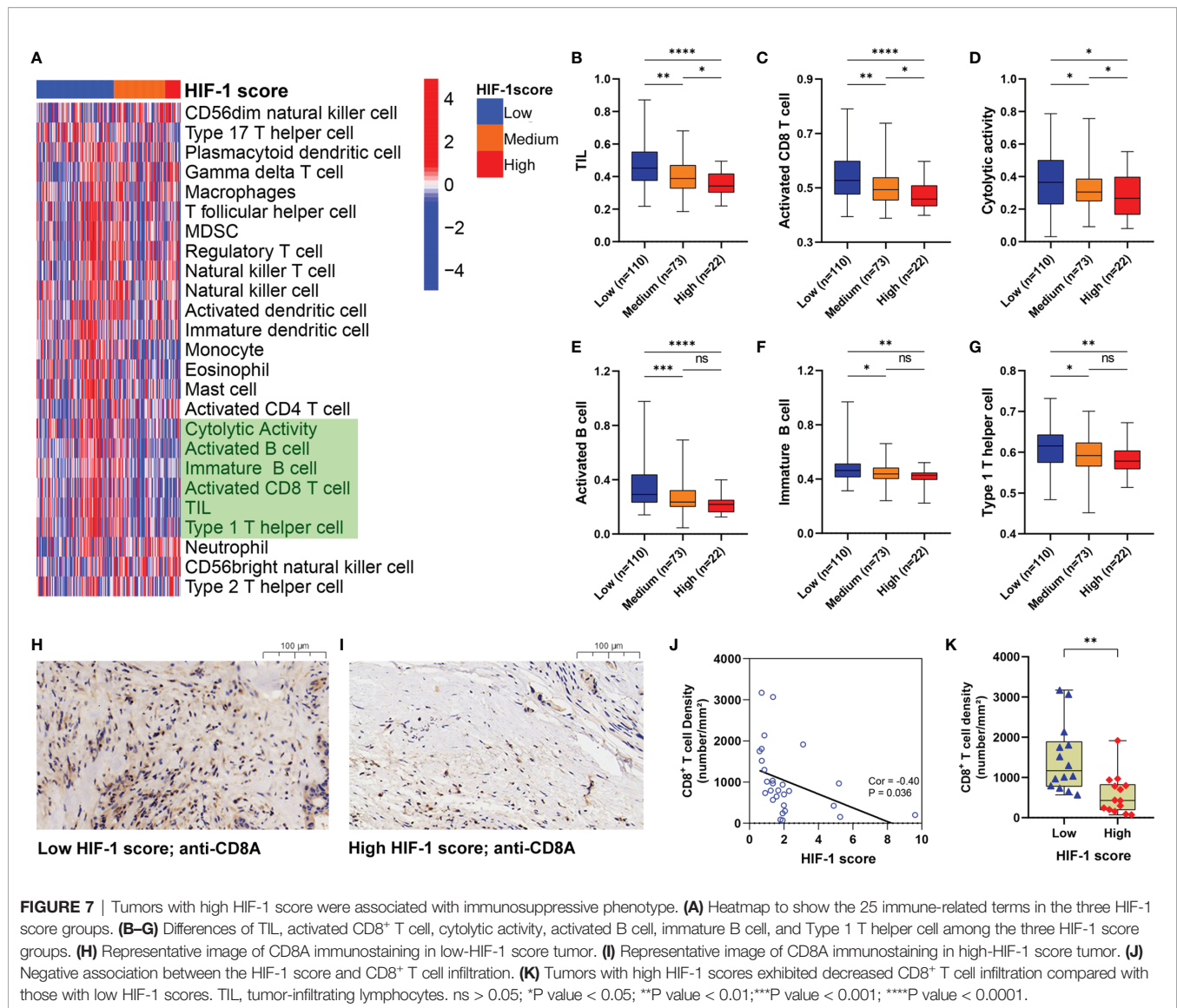


significantly to treatment failure of chemotherapy, target therapy, and immunotherapy (46–50). Targeting tumor hypoxia and HIF-1 signaling might be a promising approach to improve the therapeutic response of chemotherapies or immunotherapies for patients with PDAC. However, a previous study by J. Board et al. found no survival improvement with the combination treatment of a hypoxia inhibitor (TH-302) with gemcitabine in advanced PDAC (51). The disappointing results might be due to several reasons, including not recruiting appropriate patients because they did not check the hypoxic status of the PDAC before treatment. Therefore, to facilitate clinicians in individualized treatment decisions, it is of great value to develop a prognostic classifier to assess the hypoxic status and the corresponding molecular profile of PDAC.

In the present study, based on the known 16 HIF-1 related genes, we constructed a consensus clustering analysis to classify PDAC patients from the meta-PDAC cohort into three HIF-1 clusters. We then developed an HIF-1 score system integrated with nine prognosis-associated ODEGs among the three HIF-1 clusters, which showed reliable predictive efficacy for OS of PDAC patients through KM survival analysis, C-indexes, and AUC of

the ROC curves in the training cohort and validation cohorts. In addition, by comparing our HIF-1 score system with other hypoxia score systems established based on other cancer types, we found that our model had the highest prognostic predictive value in PDAC. Taken together, we developed a specific HIF-1 score system for PDAC, which reflects the hypoxic status of tumors and has satisfactory predictive value for patient prognoses.

Some of the nine genes utilized in the HIF-1 score system play critical roles in pancreatic carcinogenesis. For example, Wand et al. indicated that *ARNTL2* is involved in pancreatic carcinogenesis by regulating the TGF- β signaling pathway (52). *IGF2BP2* overexpression promotes PDAC progression through the PI3K/Akt signaling pathway (53). *TPX2* is a critical target of the KRAS signaling pathway and a potential therapeutic target in PDAC (54, 55). Parameswaran et al. demonstrated that *FAM83A* overexpression promotes tumor progression through the MEK-ERK signaling pathway in PDAC (56). *DCBLD2* and *DSG* were identified as unfavorable prognostic biomarkers in PDAC (57, 58). Notably, it has been reported that *FOXMI* is overexpressed in hypoxic cancer cells, which is mediated by HIF-1 (59). Cui



et al. also demonstrated that *FOXM1* impelled the Warburg effect and tumor progression in PDAC through transcriptional modulation of LDHA expression, indicating that *FOXM1* is a HIF-1 target affecting PDAC metabolism and progression (60). It should be pointed out, based on the method of data mining, that all the nine genes of our model should be HIF-1-related genes. However, many of them have not been reported to be directly regulated by HIF-1. Further studies are needed to investigate how HIF regulates or interacts with these genes.

In our study, we classified pancreatic cancer patients into three groups based on HIF-1 score system, which were HIF-1 low, medium, and high score groups. Compared to HIF-1 low and medium score groups, pancreatic cancers with HIF-1 high scores are considered more aggressive and refractory because they are associated with worse survival and more advanced grade. By exploring the molecular profile between tumors in HIF-1 low, medium, and high score groups, we found significant

enrichment of the MYC and mTORC pathways in the HIF-1 high score group. MYC has been identified as one of the main drivers of PDAC initiation and metastasis (61). Pre-clinical studies have found that inhibition of c-MYC induces cell cycle arrest and chemosensitivity and impairs hypoxia signaling in PDAC (62–65). The mTORC1 pathway is also an oncogenic signaling pathway involved in the proliferation of tumor cells through the modulation of autophagy and angiogenesis (66). Of note, a previous studies revealed that mTORC1 upregulated the transcription and translation of HIF-1 (67–69). Everolimus, an inhibitor of mTORC1, has been shown to impair tumor progression in gemcitabine-resistant PDAC by diminishing the Warburg effect (70). However, Wolpin et al. demonstrated that daily everolimus administered as a single agent had little clinical efficacy in patients with gemcitabine-resistant PDAC (71). Similarly, the combination of everolimus with cytotoxic therapies (e.g., gemcitabine and cisplatin) also failed to achieve

meaningful therapeutic responses in patients with PDAC (72–74). These results suggest that single-target therapy may not be sufficient for the eradication of pancreatic cancer cells, especially for refractory and chemoresistant cancer cells. Therefore, combination target therapy may be a promising treatment. Our findings indicate that MYC and mTORC pathways are critical driver in HIF-1 high score tumors, which provides a preliminary rationale for combination treatment using HIF-1 inhibitor and MYC inhibitor, or using HIF-1 inhibitor and everolimus in these highly hypoxic and aggressive pancreatic cancers in future studies.

In addition to activation of MYC and mTORC signaling, we revealed that pancreatic cancers with HIF-1 high scores were more immunosuppressive by further investigation into the hypoxia-immune profiles. In particular, tumors with high HIF-1 scores were associated with low infiltration of TILs, including active CD8⁺ T cells, active and immature B cells, and type 1 helper T cells. These tumors had high expression of PD-L1 and B7-H3, which are important immune checkpoint proteins. Tumor hypoxia and HIF-1 activation regulate many processes of anti-tumor immunity, leading to impaired immune responses and immune evasion (75–78). For example, HIF-1 decreases the production of IL2 and IFN- γ by CD8⁺ T cells, thereby diminishing the cytolytic activity (75). Hypoxia-mediated ROS also results in immunosuppressive and even lethal toxicity in CD8⁺ T cells (76). Interestingly, using a genetic animal model, Lee et al. demonstrated accumulation of HIF-1 α in early pancreatic neoplasia but HIF-1 α deletion accelerates PDAC initiation by increasing B cell infiltration, suggesting the pro-neoplastic effect of B cells (79). However, the role of B cells in anti-tumor immunity is still controversial (80, 81). Therefore, further studies are needed to clarify the role of B cell immunity in human PDAC and its interaction with HIF-1. Notably, hypoxia-mediated HIF-1 increases the expression of PD-L1 in multiple solid tumors through PTEN/PI3K signaling, thereby inducing anergy or apoptosis of T cells (78, 82, 83). In addition, we found that a higher HIF-1 score was also observed in the squamous tumor subtype defined by Bailey et al., which was characterized by enrichment for hypoxia response, metabolic reprogramming, and MYC signaling and associated with poor prognosis and limited immune infiltration (36). Taken together, pancreatic cancers with higher HIF-1 scores have a more immunosuppressive TME. Tumors with low/medium HIF-1 scores tend to be good candidates for immunotherapy, especially single treatment with PD-1/PD-L1 inhibitor. For highly hypoxic and immunogenic cold tumors, strategies to break immune-cell infiltrating barriers by inhibiting HIF-1 or reducing desmoplasia may be beneficial for strengthening the efficacy of immunotherapy.

Several limitations of the current study should be noticed. First, a multi-cent and large cohort should be performed to validate the prognostic prediction ability of the HIF-1 score system. Second, further experiment studies should be conducted to investigate the underlying mechanisms by which the HIF-1 related genes regulate anti-tumor immunity in PDAC.

In summary, our study established a specific HIF-1 score system to discriminate pancreatic cancers with various degrees of hypoxia status and immunosuppressive TMEs, which provides

accurate predictive value for patient prognoses. In addition, we present distinctive molecular profiles and critical oncogenic pathways for tumors with low/medium HIF-1 scores and high HIF-1 scores, which provide distinctive strategies for treating these pancreatic cancers individually.

DATA AVAILABILITY STATEMENT

The original contributions presented in the study are included in the article/**Supplementary Material**. Further inquiries can be directed to the corresponding authors.

ETHICS STATEMENT

The study was reviewed and approved by the Ethics Committee of Guangdong Provincial People's Hospital. The patients/participants provided their written informed consent to participate in this study.

AUTHOR CONTRIBUTIONS

Conceptualization: HZ, BH, YC, and CZ. Methodology: HZ, BC, and SW. Investigation: HZ, SW, ZDZ, and BC. Writing – original draft: HZ and CZ. Writing – review and editing: HZ, SW, ZDZ, ZM, ZL, CL, ZXZ, YG, and SH. Visualization: HZ. Supervision: HZ, SW, BC, SH, BH, and CZ. Funding acquisition: BC, BH, and CZ. All authors contributed to the article and approved the submitted version.

FUNDING

This study was supported by National Natural Science Foundation of China (NO.: 82072637, 82072635, 81672475 and 81702783), High-level Hospital Construction Project (DFJH201921), and Fundamental Research Funds for the Central Universities (y2syD2192230).

ACKNOWLEDGMENTS

The authors would like to give their sincere appreciation to the reviewers for their helpful comments on this article and research groups for the TCGA and CEO, which provided data for this collection.

SUPPLEMENTARY MATERIAL

The Supplementary Material for this article can be found online at: <https://www.frontiersin.org/articles/10.3389/fimmu.2021.790661/full#supplementary-material>

Supplementary Figure 1 | (A) Differential expression analysis of the 16 HIF-1 related genes between non-tumor and tumor samples. **(B)** Forest plots to show the results of KM survival analysis of the 16 HIF-1 related genes. KM, Kaplan-Meier. **P value < 0.01; ***P value < 0.001; ****P value < 0.0001.

Supplementary Figure 2 | (A) Differential expression analysis between HIF-1 cluster **(A, B)**. **(B)** Differential expression analysis between HIF-1 cluster **(A, C)**. **(C)** Differential expression analysis between HIF-1 cluster **(B, C)**. **(D)** Intersection of differential expressed genes among these three HIF-1 clusters.

Supplementary Figure 3 | Heatmaps to show the top 20 differential oncologic biological pathways and metabolic processes between different HIF-1 score groups were respectively presented using heatmaps.

Supplementary Figure 4 | (A) Association between HIF-1 score and PD-L1 expression in PDAC. **(B)** Association between HIF-1 score and B7-H3 expression in PDAC. **(C)** Patients in patients in squamous subtype had significant higher HIF-1 score than those in immunogenic subtype. PDAC, pancreatic ductal adenocarcinoma. ****P value < 0.0001.

REFERENCES

- Mizrahi JD, Surana R, Valle JW, Shroff RT. Pancreatic Cancer. *Lancet* (2020) 395:2008–20. doi: 10.1016/S0140-6736(20)30974-0
- McGuigan A, Kelly P, Turkington RC, Jones C, Coleman HG, McCain RS. Pancreatic Cancer: A Review of Clinical Diagnosis, Epidemiology, Treatment and Outcomes. *World J Gastroenterol* (2018) 24:4846–61. doi: 10.3748/wjg.v24.i43.4846
- Neoptolemos JP, Kleeff J, Michl P, Costello E, Greenhalf W, Palmer DH. Therapeutic Developments in Pancreatic Cancer: Current and Future Perspectives. *Nat Rev Gastroenterol Hepatol* (2018) 15:333–48. doi: 10.1038/s41575-018-0005-x
- Elailah A, Saharia A, Potter L, Baio F, Ghafel A, Abdelrahim M, et al. Promising New Treatments for Pancreatic Cancer in the Era of Targeted and Immune Therapies. *Am J Cancer Res* (2019) 9:1871–88.
- Kowalewski A, Szyllberg L, Saganek M, Napiontek W, Antosik P, Grzanka D. Emerging Strategies in BRCA-Positive Pancreatic Cancer. *J Cancer Res Clin Oncol* (2018) 144:1503–7. doi: 10.1007/s00432-018-2666-9
- Furuse J. A PARP Inhibitor in Pancreatic Cancer: Enhancement Anti-Tumour Activity of Chemoradiation Therapy Against Pancreatic Cancer? *EBioMedicine* (2019) 40:9–10. doi: 10.1016/j.ebiom.2019.01.039
- Kaufman B, Shapira-Frommer R, Schmutzler RK, Audeh MW, Friedlander M, Balmana J, et al. Olaparib Monotherapy in Patients With Advanced Cancer and a Germline BRCA1/2 Mutation. *J Clin Oncol* (2015) 33:244–50. doi: 10.1200/JCO.2014.56.2728
- Zhu H, Wei M, Xu J, Hua J, Liang C, Meng Q, et al. PARP Inhibitors in Pancreatic Cancer: Molecular Mechanisms and Clinical Applications. *Mol Cancer* (2020) 19:49. doi: 10.1186/s12943-020-01167-9
- Wang BC, Li PC, Fan JQ, Lin GH, Liu Q. Durvalumab and Tremelimumab Combination Therapy Versus Durvalumab or Tremelimumab Monotherapy for Patients With Solid Tumors: A Systematic Review and Meta-Analysis. *Med (Baltimore)* (2020) 99:e21273. doi: 10.1097/MD.00000000000021273
- O'Reilly EM, Oh DY, Dhani N, Renouf DJ, Lee MA, Sun W, et al. Durvalumab With or Without Tremelimumab for Patients With Metastatic Pancreatic Ductal Adenocarcinoma: A Phase 2 Randomized Clinical Trial. *JAMA Oncol* (2019) 5:1431–8. doi: 10.1001/jamaoncol.2019.1588
- Ho WJ, Jaffee EM, Zheng L. The Tumour Microenvironment in Pancreatic Cancer - Clinical Challenges and Opportunities. *Nat Rev Clin Oncol* (2020) 17:527–40. doi: 10.1038/s41571-020-0363-5
- Torphy RJ, Schulick RD, Zhu Y. Understanding the Immune Landscape and Tumor Microenvironment of Pancreatic Cancer to Improve Immunotherapy. *Mol Carcinog* (2020) 59:775–82. doi: 10.1002/mc.23179
- Tao J, Yang G, Zhou W, Qiu J, Chen G, Luo W, et al. Targeting Hypoxic Tumor Microenvironment in Pancreatic Cancer. *J Hematol Oncol* (2021) 14:14. doi: 10.1186/s13045-020-01030-w
- Liu L, Xu HX, He M, Wang W, Wang WQ, Wu CT, et al. A Novel Scoring System Predicts Postsurgical Survival and Adjuvant Chemotherapeutic Benefits in Patients With Pancreatic Adenocarcinoma: Implications for AJCC-TNM Staging. *Surg* (2018) 163:1280–94. doi: 10.1016/j.surg.2018.01.017
- Yan X, Wan H, Hao X, Lan T, Li W, Xu L, et al. Importance of Gene Expression Signatures in Pancreatic Cancer Prognosis and the Establishment of a Prediction Model. *Cancer Manag Res* (2019) 11:273–83. doi: 10.2147/CMAR.S185205
- Liu ZQ, Xiao ZW, Luo GP, Liu L, Liu C, Xu J, et al. Effect of the Number of Positive Lymph Nodes and Lymph Node Ratio on Prognosis of Patients After Resection of Pancreatic Adenocarcinoma. *Hepatobiliary Pancreat Dis Int* (2014) 13:634–41. doi: 10.1016/s1499-3872(14)60264-2
- Sada M, Ohuchida K, Horioka K, Okumura T, Moriyama T, Miyasaka Y, et al. Hypoxic Stellate Cells of Pancreatic Cancer Stroma Regulate Extracellular Matrix Fiber Organization and Cancer Cell Motility. *Cancer Lett* (2016) 372:210–8. doi: 10.1016/j.canlet.2016.01.016
- Mangge H, Niedrist T, Renner W, Lyer S, Alexiou C, Haybaeck J. New Diagnostic and Therapeutic Aspects of Pancreatic Ductal Adenocarcinoma. *Curr Med Chem* (2017) 24:3012–24. doi: 10.2174/0929867324666170510150124
- Sharbeen G, McCarroll JA, Akerman A, Kopecky C, Youkhana J, Kokkinos J, et al. Cancer-Associated Fibroblasts in Pancreatic Ductal Adenocarcinoma Determine Response to SLC7A11 Inhibition. *Cancer Res* (2021) 18:3461. doi: 10.1158/0008-5472.CAN-20-2496
- Duffy JP, Eibl G, Reber HA, Hines OJ. Influence of Hypoxia and Neovascularization on the Growth of Pancreatic Cancer. *Mol Cancer* (2003) 2:12. doi: 10.1186/1476-4598-2-12
- Shah VM, Sheppard BC, Sears RC, Alani AW. Hypoxia: Friend or Foe for Drug Delivery in Pancreatic Cancer. *Cancer Lett* (2020) 492:63–70. doi: 10.1016/j.canlet.2020.07.041
- Zhu GH, Huang C, Feng ZZ, Lv XH, Qiu ZJ. Hypoxia-Induced Snail Expression Through Transcriptional Regulation by HIF-1 α in Pancreatic Cancer Cells. *Dig Dis Sci* (2013) 58:3503–15. doi: 10.1007/s10620-013-2841-4
- Yang SY, Song BQ, Dai SL, Yang KX, Jin Z, Shi KW. Effects of Hypoxia-Inducible Factor-1 α Silencing on Drug Resistance of Human Pancreatic Cancer Cell Line Patu8988/5-Fu. *Hepatogastroenterol* (2014) 61:2395–401.
- You L, Wu W, Wang X, Fang L, Adam V, Nepovimova E, et al. The Role of Hypoxia-Inducible Factor 1 in Tumor Immune Evasion. *Med Res Rev* (2021) 41:1622–43. doi: 10.1002/med.21771
- Noman MZ, Desantis G, Janji B, Hasmmim M, Karray S, Dessen P, et al. PD-L1 Is a Novel Direct Target of HIF-1 α , and Its Blockade Under Hypoxia Enhanced MDSC-Mediated T Cell Activation. *J Exp Med* (2014) 211:781–90. doi: 10.1084/jem.20131916
- Samanta D, Park Y, Ni X, Li H, Zahnow CA, Gabrielson E, et al. Chemotherapy Induces Enrichment of CD47(+)/CD73(+)/PDL1(+) Immune Evasive Triple-Negative Breast Cancer Cells. *Proc Natl Acad Sci USA* (2018) 115:E1239–48. doi: 10.1073/pnas.1718197115
- Zhang H, Lu H, Xiang L, Bullen JW, Zhang C, Samanta D, et al. HIF-1 Regulates CD47 Expression in Breast Cancer Cells to Promote Evasion of Phagocytosis and Maintenance of Cancer Stem Cells. *Proc Natl Acad Sci USA* (2015) 112:E6215–23. doi: 10.1073/pnas.1520032112
- Semenza GL. HIF-1: Upstream and Downstream of Cancer Metabolism. *Curr Opin Genet Dev* (2010) 20:51–6. doi: 10.1016/j.gde.2009.10.009
- Deng F, Chen D, Wei X, Lu S, Luo X, He J, et al. Development and Validation of a Prognostic Classifier Based on HIF-1 Signaling for Hepatocellular Carcinoma. *Aging (Albany NY)* (2020) 12:3431–50. doi: 10.18632/aging.102820
- Camp RL, Dolled-Filhart M, Rimm DL. X-Tile: A New Bio-Informatics Tool for Biomarker Assessment and Outcome-Based Cut-Point Optimization. *Clin Cancer Res* (2004) 10:7252–9. doi: 10.1158/1078-0432.CCR-04-0713
- Hanzelmann S, Castelo R, Guinney J. GSEA: Gene Set Variation Analysis for Microarray and RNA-Seq Data. *BMC Bioinf* (2013) 14:7. doi: 10.1186/1471-2105-14-7
- Bindea G, Mlecnik B, Tosolini M, Kirilovsky A, Waldner M, Obenauf AC, et al. Spatiotemporal Dynamics of Intratumoral Immune Cells Reveal the Immune Landscape in Human Cancer. *Immunity* (2013) 39:782–95. doi: 10.1016/j.immuni.2013.10.003

33. Buffa FM, Harris AL, West CM, Miller CJ. Large Meta-Analysis of Multiple Cancers Reveals a Common, Compact and Highly Prognostic Hypoxia Metagene. *Br J Cancer* (2010) 102:428–35. doi: 10.1038/sj.bjc.6605450
34. Ragnun HB, Vlatkovic L, Lie AK, Axcrone K, Julin CH, Frikstad KM, et al. The Tumour Hypoxia Marker Pimonidazole Reflects a Transcriptional Programme Associated With Aggressive Prostate Cancer. *Br J Cancer* (2015) 112:382–90. doi: 10.1038/bjc.2014.604
35. Winter SC, Buffa FM, Silva P, Miller C, Valentine HR, Turley H, et al. Relation of a Hypoxia Metagene Derived From Head and Neck Cancer to Prognosis of Multiple Cancers. *Cancer Res* (2007) 67:3441–9. doi: 10.1158/0008-5472.CAN-06-3322
36. Bailey P, Chang DK, Nones K, Johns AL, Patch AM, Gingras MC, et al. Genomic Analyses Identify Molecular Subtypes of Pancreatic Cancer. *Nat* (2016) 531:47–52. doi: 10.1038/nature16965
37. Yamasaki A, Yanai K, Onishi H. Hypoxia and Pancreatic Ductal Adenocarcinoma. *Cancer Lett* (2020) 484:9–15. doi: 10.1016/j.canlet.2020.04.018
38. Biancur DE, Kimmelman AC. The Plasticity of Pancreatic Cancer Metabolism in Tumor Progression and Therapeutic Resistance. *Biochim Biophys Acta Rev Cancer* (2018) 1870:67–75. doi: 10.1016/j.bbcan.2018.04.011
39. Espiau-Romera P, Courtois S, Parejo-Alonso B, Sancho P. Molecular and Metabolic Subtypes Correspondence for Pancreatic Ductal Adenocarcinoma Classification. *J Clin Med* (2020) 9:4128. doi: 10.3390/jcm9124128
40. Fournel L, Wu Z, Stadler N, Damotte D, Lococo F, Boulle G, et al. Cisplatin Increases PD-L1 Expression and Optimizes Immune Check-Point Blockade in Non-Small Cell Lung Cancer. *Cancer Lett* (2019) 464:5–14. doi: 10.1016/j.canlet.2019.08.005
41. Fu Y, Liu S, Zeng S, Shen H. From Bench to Bed: The Tumor Immune Microenvironment and Current Immunotherapeutic Strategies for Hepatocellular Carcinoma. *J Exp Clin Cancer Res* (2019) 38:396. doi: 10.1186/s13046-019-1396-4
42. Ridolfi L, De Rosa F, Petracchi E, Tanda ET, Marra E, Pigozzo J, et al. Anti-PD1 Antibodies in Patients Aged \geq 75 Years With Metastatic Melanoma: A Retrospective Multicentre Study. *J Geriatr Oncol* (2020) 11. doi: 10.1016/j.jgo.2019.12.012
43. Hou YC, Chao YJ, Hsieh MH, Tung HL, Wang HC, Shan YS. Low CD8(+) T Cell Infiltration and High PD-L1 Expression Are Associated With Level of CD44(+)/CD133(+) Cancer Stem Cells and Predict an Unfavorable Prognosis in Pancreatic Cancer. *Cancers (Basel)* (2019) 11:541. doi: 10.3390/cancers11040541
44. Li J, Yuan S, Norgard RJ, Yan F, Yamazoe T, Blanco A, et al. Tumor Cell-Intrinsic USP22 Suppresses Antitumor Immunity in Pancreatic Cancer. *Cancer Immunol Res* (2019) 8:282–91. doi: 10.1158/2326-6066.CIR-19-0661
45. Balachandran VP, Beatty GL, Dougan SK. Broadening the Impact of Immunotherapy to Pancreatic Cancer: Challenges and Opportunities. *Gastroenterol* (2019) 156:2056–72. doi: 10.1053/j.gastro.2018.12.038
46. Shukla SK, Purohit V, Mehla K, Gunda V, Chaika NV, Vernucci E, et al. MUC1 and HIF-1 α Signaling Crosstalk Induces Anabolic Glucose Metabolism to Impart Gemcitabine Resistance to Pancreatic Cancer. *Cancer Cell* (2017) 32:71–87 e7. doi: 10.1016/j.ccell.2017.06.004
47. Ma J, Weng L, Jia Y, Liu B, Wu S, Xue L, et al. PTBP3 Promotes Malignancy and Hypoxia-Induced Chemoresistance in Pancreatic Cancer Cells by ATG12 Up-Regulation. *J Cell Mol Med* (2020) 24:2917–30. doi: 10.1111/jcmm.14896
48. Daniel SK, Sullivan KM, Labadie KP, Pillarisetty VG. Hypoxia as a Barrier to Immunotherapy in Pancreatic Adenocarcinoma. *Clin Transl Med* (2019) 8:10. doi: 10.1186/s40169-019-0226-9
49. Yang X, Lu Y, Hang J, Zhang J, Zhang T, Huo Y, et al. Lactate-Modulated Immunosuppression of Myeloid-Derived Suppressor Cells Contributes to the Radioresistance of Pancreatic Cancer. *Cancer Immunol Res* (2020) 8:1440–51. doi: 10.1158/2326-6066.CIR-20-0111
50. Luo W, Qiu J, Zheng L, Zhang T. Novel Therapies Targeting Hypoxia Mechanism to Treat Pancreatic Cancer. *Chin J Cancer Res* (2021) 33:216–31. doi: 10.21147/j.issn.1000-9604.2021.02.09
51. Borad MJ, Reddy SG, Bahary N, Uronis HE, Sigal D, Cohn AL, et al. Randomized Phase II Trial of Gemcitabine Plus TH-302 Versus Gemcitabine in Patients With Advanced Pancreatic Cancer. *J Clin Oncol* (2015) 33:1475–81. doi: 10.1200/JCO.2014.55.7504
52. Wang Z, Liu T, Xue W, Fang Y, Chen X, Xu L, et al. ARNTL2 Promotes Pancreatic Ductal Adenocarcinoma Progression Through TGF/ β Pathway and Is Regulated by miR-26a-5p. *Cell Death Dis* (2020) 11:692. doi: 10.1038/s41419-020-02839-6
53. Xu X, Yu Y, Zong K, Lv P, Gu Y. Up-Regulation of IGF2BP2 by Multiple Mechanisms in Pancreatic Cancer Promotes Cancer Proliferation by Activating the PI3K/Akt Signaling Pathway. *J Exp Clin Cancer Res* (2019) 38:497. doi: 10.1186/s13046-019-1470-y
54. Warner SL, Stephens BJ, Nwokenkwo S, Hostetter G, Sugeng A, Hidalgo M, et al. Validation of TPX2 as a Potential Therapeutic Target in Pancreatic Cancer Cells. *Clin Cancer Res* (2009) 15:6519–28. doi: 10.1158/1078-0432.CCR-09-0077
55. Gomes-Filho SM, Dos Santos EO, Bertoldi ERM, Scalabrini LC, Heidrich V, Dazzani B, et al. Aurora A Kinase and Its Activator TPX2 Are Potential Therapeutic Targets in KRAS-Induced Pancreatic Cancer. *Cell Oncol (Dordr)* (2020) 43:445–60. doi: 10.1007/s13402-020-00498-5
56. Parameswaran N, Bartel CA, Hernandez-Sanchez W, Miskimen KL, Smigiel JM, Khalil AM, et al. A FAM83A Positive Feed-Back Loop Drives Survival and Tumorigenicity of Pancreatic Ductal Adenocarcinomas. *Sci Rep* (2019) 9:13396. doi: 10.1038/s41598-019-49475-5
57. Feng Z, Li K, Wu Y, Peng C. Transcriptomic Profiling Identifies DCBLD2 as a Diagnostic and Prognostic Biomarker in Pancreatic Ductal Adenocarcinoma. *Front Mol Biosci* (2021) 8:659168. doi: 10.3389/fmolb.2021.659168
58. Ormanns S, Altendorf-Hofmann A, Jackstadt R, Horst D, Assmann G, Zhao Y, et al. Desmogleins as Prognostic Biomarkers in Resected Pancreatic Ductal Adenocarcinoma. *Br J Cancer* (2015) 113:1460–6. doi: 10.1038/bjc.2015.362
59. Xia LM, Huang WJ, Wang B, Liu M, Zhang Q, Yan W, et al. Transcriptional Up-Regulation of FoxM1 in Response to Hypoxia Is Mediated by HIF-1. *J Cell Biochem* (2009) 106:247–56. doi: 10.1002/jcb.21996
60. Cui J, Shi M, Xie D, Wei D, Jia Z, Zheng S, et al. FOXM1 Promotes the Warburg Effect and Pancreatic Cancer Progression via Transactivation of LDHA Expression. *Clin Cancer Res* (2014) 20:2595–606. doi: 10.1158/1078-0432.CCR-13-2407
61. Ischenko I, Petrenko O, Hayman MJ. Analysis of the Tumor-Initiating and Metastatic Capacity of PDX1-Positive Cells From the Adult Pancreas. *Proc Natl Acad Sci USA* (2014) 111:3466–71. doi: 10.1073/pnas.1319911111
62. Liu X, Zhou Y, Peng J, Xie B, Shou Q, Wang J. Silencing C-Myc Enhances the Antitumor Activity of Bufalin by Suppressing the HIF-1 α /SDF-1/CXCR4 Pathway in Pancreatic Cancer Cells. *Front Pharmacol* (2020) 11:495. doi: 10.3389/fphar.2020.00495
63. Liu X, Xiao XY, Shou QY, Yan JF, Chen L, Fu HY, et al. Bufalin Inhibits Pancreatic Cancer by Inducing Cell Cycle Arrest via the C-Myc/NF- κ B Pathway. *J Ethnopharmacol* (2016) 193:538–45. doi: 10.1016/j.jep.2016.09.047
64. Chien W, Lee DH, Zheng Y, Wuenschel P, Alvarez R, Wen DL, et al. Growth Inhibition of Pancreatic Cancer Cells by Histone Deacetylase Inhibitor Belinostat Through Suppression of Multiple Pathways Including HIF, NF κ B, and mTOR Signaling *In Vitro* and *In Vivo*. *Mol Carcinog* (2014) 53:722–35. doi: 10.1002/mc.22024
65. Zhang M, Fan HY, Li SC. Inhibition of C-Myc by 10058-F4 Induces Growth Arrest and Chemoresensitivity in Pancreatic Ductal Adenocarcinoma. *BioMed Pharmacother* (2015) 73:123–8. doi: 10.1016/j.biopha.2015.05.019
66. Babiker HM, Karass M, Recio-Boiles A, Chandana SR, McBride A, Mahadevan D. Everolimus for the Treatment of Advanced Pancreatic Ductal Adenocarcinoma (PDAC). *Expert Opin Investig Drugs* (2019) 28:583–92. doi: 10.1080/13543784.2019.1632289
67. Semenza GL. Targeting HIF-1 for Cancer Therapy. *Nat Rev Cancer* (2003) 3:721–32. doi: 10.1038/nrc1187
68. Wang Y, Zhao Q, Ma S, Yang F, Gong Y, Ke C. Sirolimus Inhibits Human Pancreatic Carcinoma Cell Proliferation by a Mechanism Linked to the Targeting of mTOR/HIF-1 α /VEGF Signaling. *IUBMB Life* (2007) 59:717–21. doi: 10.1080/15216540701646484
69. Huang C, Li Y, Li Z, Xu Y, Li N, Ge Y, et al. LIMS1 Promotes Pancreatic Cancer Cell Survival Under Oxygen-Glucose Deprivation Conditions by Enhancing HIF1A Protein Translation. *Clin Cancer Res* (2019) 25:4091–103. doi: 10.1158/1078-0432.CCR-18-3533
70. Cui J, Guo Y, Wu H, Xiong J, Peng T. Everolimus Regulates the Activity of Gemcitabine-Resistant Pancreatic Cancer Cells by Targeting the Warburg Effect via PI3K/AKT/mTOR Signaling. *Mol Med* (2021) 27:38. doi: 10.1186/s10020-021-00300-8

71. Wolpin BM, Hezel AF, Abrams T, Blaszkowsky LS, Meyerhardt JA, Chan JA, et al. Oral mTOR Inhibitor Everolimus in Patients With Gemcitabine-Refractory Metastatic Pancreatic Cancer. *J Clin Oncol* (2009) 27:193–8. doi: 10.1200/JCO.2008.18.9514
72. Costello BA, Borad MJ, Qi Y, Kim GP, Northfelt DW, Erlichman C, et al. Phase I Trial of Everolimus, Gemcitabine and Cisplatin in Patients With Solid Tumors. *Invest New Drugs* (2014) 32:710–6. doi: 10.1007/s10637-014-0096-3
73. Joka M, Boeck S, Zech CJ, Seufferlein T, Wichert G, Licht T, et al. Combination of Antiangiogenic Therapy Using the mTOR-Inhibitor Everolimus and Low-Dose Chemotherapy for Locally Advanced and/or Metastatic Pancreatic Cancer: A Dose-Finding Study. *Anticancer Drugs* (2014) 25:1095–101. doi: 10.1097/CAD.0000000000000146
74. Weinberg BA, Wang H, Witkiewicz AK, Marshall JL, He AR, Vail P, et al. A Phase I Study of Ribociclib Plus Everolimus in Patients With Metastatic Pancreatic Adenocarcinoma Refractory to Chemotherapy. *J Pancreat Cancer* (2020) 6:45–54. doi: 10.1089/pancan.2020.0005
75. Caldwell CC, Kojima H, Lukashov D, Armstrong J, Farber M, Apasov SG, et al. Differential Effects of Physiologically Relevant Hypoxic Conditions on T Lymphocyte Development and Effector Functions. *J Immunol* (2001) 167:6140–9. doi: 10.4049/jimmunol.167.11.6140
76. Hildeman DA, Mitchell T, Teague TK, Henson P, Day BJ, Kappler J, et al. Reactive Oxygen Species Regulate Activation-Induced T Cell Apoptosis. *Immunol* (1999) 10:735–44. doi: 10.1016/s1074-7613(00)80072-2
77. Chen J, Jiang CC, Jin L, Zhang XD. Regulation of PD-L1: A Novel Role of Pro-Survival Signalling in Cancer. *Ann Oncol* (2016) 27:409–16. doi: 10.1093/annonc/mdv615
78. Barsoum IB, Smallwood CA, Siemens DR, Graham CH. A Mechanism of Hypoxia-Mediated Escape From Adaptive Immunity in Cancer Cells. *Cancer Res* (2014) 74:665–74. doi: 10.1158/0008-5472.CAN-13-0992
79. Lee KE, Spata M, Bayne LJ, Buza EL, Durham AC, Allman D, et al. Hif1a Deletion Reveals Pro-Neoplastic Function of B Cells in Pancreatic Neoplasia. *Cancer Discov* (2016) 6:256–69. doi: 10.1158/2159-8290.CD-15-0822
80. Wouters MCA, Nelson BH. Prognostic Significance of Tumor-Infiltrating B Cells and Plasma Cells in Human Cancer. *Clin Cancer Res* (2018) 24:6125–35. doi: 10.1158/1078-0432.CCR-18-1481
81. Pineda S, Lopez de Maturana E, Yu K, Ravoor A, Wood I, Malats N, et al. Tumor-Infiltrating B- and T-Cell Repertoire in Pancreatic Cancer Associated With Host and Tumor Features. *Front Immunol* (2021) 12:730746. doi: 10.3389/fimmu.2021.730746
82. Parsa AT, Waldron JS, Panner A, Crane CA, Parney IF, Barry JJ, et al. Loss of Tumor Suppressor PTEN Function Increases B7-H1 Expression and Immunoresistance in Glioma. *Nat Med* (2007) 13:84–8. doi: 10.1038/nm1517
83. Dong H, Strome SE, Salomao DR, Tamura H, Hirano F, Flies DB, et al. Tumor-Associated B7-H1 Promotes T-Cell Apoptosis: A Potential Mechanism of Immune Evasion. *Nat Med* (2002) 8:793–800. doi: 10.1038/nm730

Conflict of Interest: The authors declare that the research was conducted in the absence of any commercial or financial relationships that could be construed as a potential conflict of interest.

Publisher's Note: All claims expressed in this article are solely those of the authors and do not necessarily represent those of their affiliated organizations, or those of the publisher, the editors and the reviewers. Any product that may be evaluated in this article, or claim that may be made by its manufacturer, is not guaranteed or endorsed by the publisher.

Copyright © 2021 Zhuang, Wang, Chen, Zhang, Ma, Li, Liu, Zhou, Gong, Huang, Hou, Chen and Zhang. This is an open-access article distributed under the terms of the Creative Commons Attribution License (CC BY). The use, distribution or reproduction in other forums is permitted, provided the original author(s) and the copyright owner(s) are credited and that the original publication in this journal is cited, in accordance with accepted academic practice. No use, distribution or reproduction is permitted which does not comply with these terms.